Electronic supplementary materials *Mendeleev Commun.*, 2024, **34**, 667–669

Octafluorobiphenyl-4,4′-diyl 9-oxothioxanthene-1,4-diyl polyether – a promising material for organic film based memristors: synthesis, memristive effect and charge transport mechanism

Inna K. Shundrina, Irina A. Os'kina, Danila S. Odintsov, Andrei A. Gismatulin, Ivan A. Azarov, Leonid A. Shundrin and Vladimir A. Gritsenko

Content

The starting compounds

The starting monomer, 1,4-dihydroxy-9*H*-thioxanthen-9-one **1** was prepared as described in ref. [S1]. Perfluorobiphenyl **2** (99.5%) was purchased from Aldrich and used without purification.

Synthesis of poly(OFB-ThS) 3

N,*N*-Dimethylacetamide (3 ml), compound **1** (280 mg, 1.148 mmol) and K_2CO_3 (316 mg, 2.296 mmol) were stirred under argon at 120 ºC for 2 h with a Dean–Stark trap whose nozzle was filled with toluene. The flask was then cooled to 80 ºC, and perfluorobiphenyl **2** (383 mg, 1.148 mmol) was added. The temperature was then raised to 110 ºC, and the reaction was allowed to continue at this temperature for 5 hours. The final reaction mixture was cooled to room temperature, and the polymer **3** was precipitated with ethanol (50 ml). The precipitate was centrifuged and washed three times with ethanol. The polymer was dried in air at 80 ºC for 24 hours. The yield of the polymer was 82%.

The ^{1}H NMR spectrum of polymer **3** showed the absence of the signals from possible terminal OH groups; aromatic protons: 6.8 <δ<8.6 ppm (broadened) (Figure S3). ^{19}F NMR spectrum, *δ*: 138.34, 139.74, 154.42, 156.42 ppm (intense) (Figure S4).

NMR spectra of compounds 1, 2 and poly(OFB-ThS) 3

Reactants:

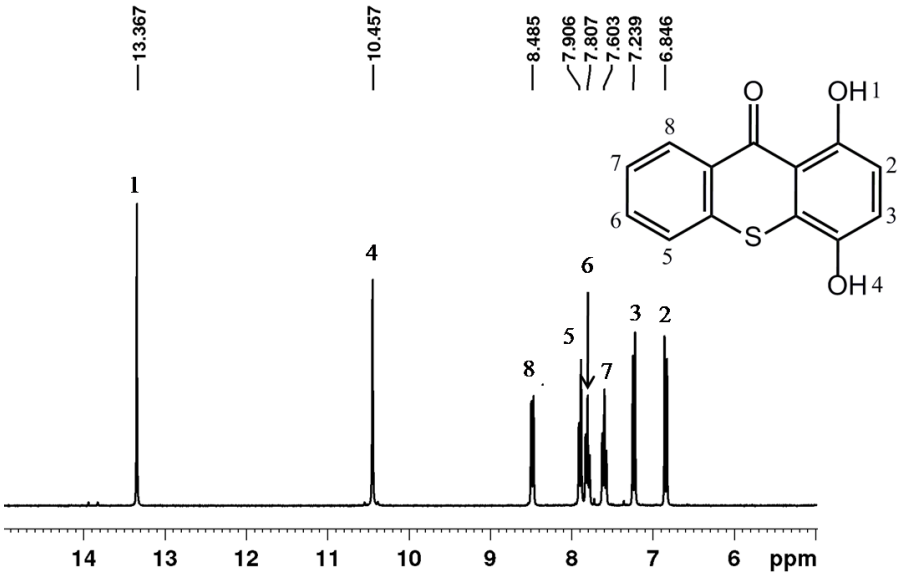

Figure S1. ^{1}H NMR spectrum of compound **1**, 600 MHz, DMSO-d_6.

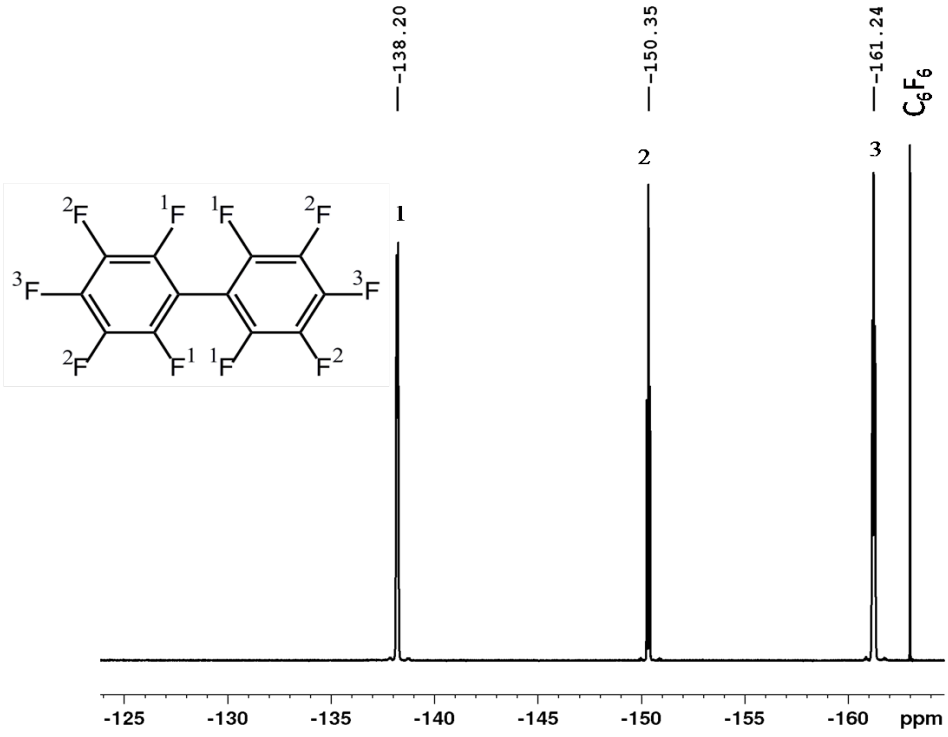

Figure S2. ^{19}F NMR spectrum of compound **2**, 600 MHz, DMSO-d_6.

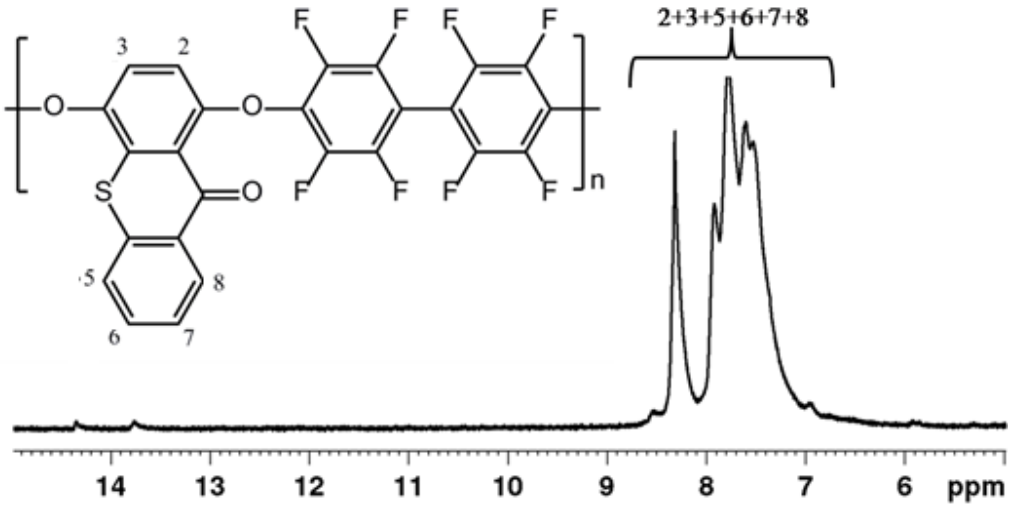

Figure S3. ^{1}H NMR spectrum of poly(OFB-ThS) **3**, 600 MHz, DMSO-d_6.

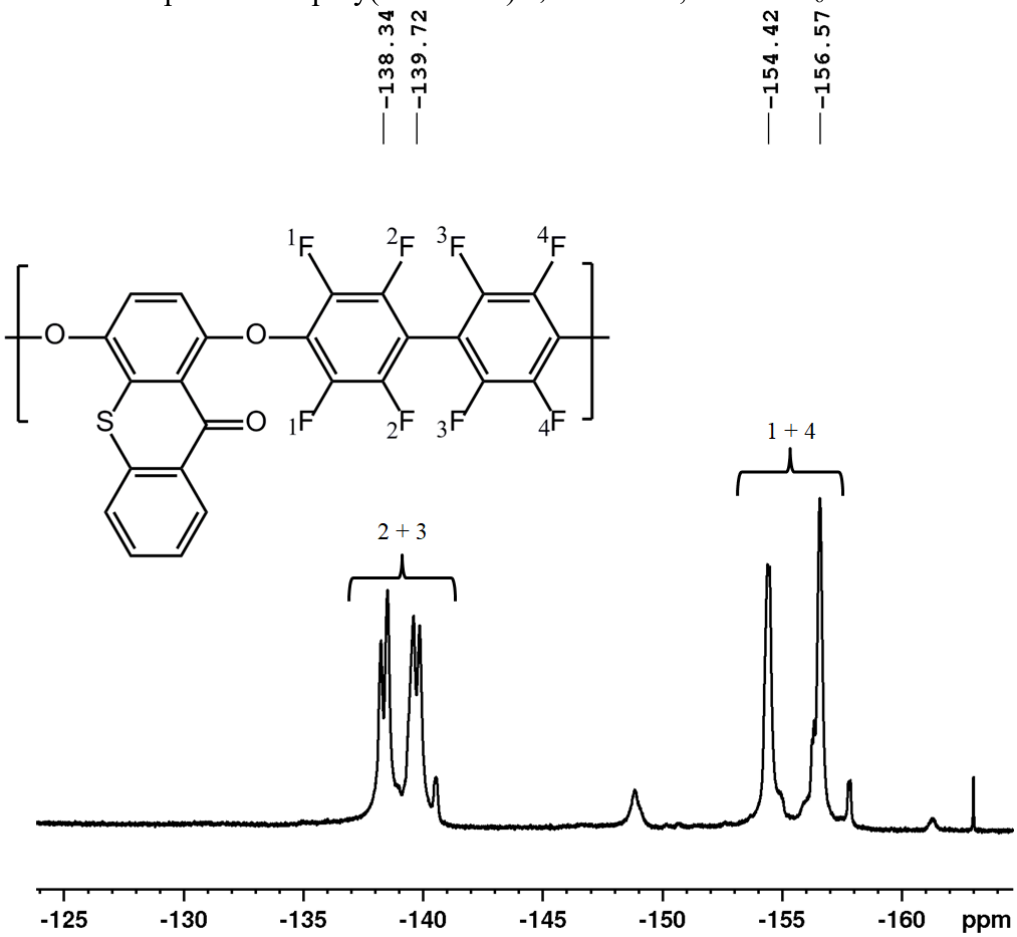

Figure S4. ^{19}F NMR spectrum of poly(OFB-ThS) **3**, 600 MHz, DMSO-d_6.

In the ^{1}H spectrum of poly(OFB-ThS) **3** the signals of the aromatic protons of the thioxanthenone fragment are broadened and appear in the range of $6.8<\delta<8.6$ ppm (Figure S3). In the ^{19}F spectrum of poly(OFB-ThS) (Figure S4), the intense signals at δ=138.34, 139.74, 154.42, 156.42 ppm are associated with fluorine nuclei in the repeating fragment of the polymer chain. The less intense signals are associated with the terminal biphenyl fragments.

Gel permeation chromatography (GPC) and thermogravimetric analysis

Molecular weight characteristics were determined by gel permeation chromatography (GPC) using an Agilent LC-1200 chromatograph (Agilent Technologies, USA) equipped with a PL 1110-6500-gel 5μm Mixed-C column. THF was used as the eluent at a flow rate of 1 mL/min at 40 °C. Polystyrene standards from Waters company (USA) were used to calibrate the chromatograph. Thermogravimetric analysis (TGA) and differential scanning calorimetry (DSC) were performed using a STA 409 synchronous thermal analyzer (Netzsch, Germany) at a heating rate of 10 °C/min. The glass transition temperature (T_g) was determined from the DSC curves as the center of the transition step in the second heating cycle in a helium flow. The results are shown in Table 1 (main text).

Electrochemical measurements

Thin layer cyclic voltammetry measurements of the poly(OFB-ThS) film were carried out at 295 K in an argon atmosphere. The supporting electrolyte was 0.1 M Et_4NClO_4. A PG 310 USB potentiostat (HEKA Elektronik GmbH, Germany) was used for the measurements. A standard electrochemical cell with a solution volume of 5 ml connected to the potentiostat with a three-electrode scheme was employed. A stationary Pt electrode (S = 0.069 cm^2) was used as the working electrode, a saturated calomel electrode (SCE) was used as the reference electrode, and a Pt helix was used as the auxiliary electrode. Onset and peak potentials (Table 1, main text) were quoted with reference to the SCE. A triangular potential sweep was used. The potential sweep rates were $\nu = 0.1\ V \cdot s^{-1}$. The surface modification of the working electrode with poly(OFB-ThS) was carried out as described in ref. [S2]. Table S1 summarises all molecular weight characteristics, thermal and electrochemical data of poly(OFB-ThS) **3**.

Table S1. Molecular weights (*kDa*), polydispersity index, glass transition (T_g) and 3% mass loss ($T_{3\%}$) temperatures[a] (°C) together with electrochemical reduction/oxidation (Red/Ox) onset and peak potentials[b] (V) of the poly(OFB-ThS) film deposited on the Pt working electrode.

M_n	M_w	PDI[c]	T_g	$T_{3\%}$	E_{onset}^{Ox}	E_p^{1A}	E_{onset}^{Red}	E_p^{1C}
7.1	24.0	3.36	247	312	1.58	1.90	–1.41	–1.71

[a] In He atmosphere. [b] The working electrode was modified by the poly(OFB-ThS) thin film as described in *Mendeleev Commun*. 2012, **22**, 111. The potentials are quoted with the reference to a saturated calomel electrode (SCE). [c] Polydispersity index (M_w/M_n).

Fabrication of MIS/MIM structures and their voltammetric measurements

The poly(OFB-ThS) polymer films were deposited from a 1% poly(OFB-ThS) **3** solution in chloroform on Si (100) p/(p^{++}) type silicon wafers and glassy ITO wafers by centrifugation using the spin-coater "spin NXG-P1AC" (India). Prior to centrifugation, the Si wafer was treated with a 10% HF solution to remove the natural oxide film. The ITO-wafer was pre-cleaned as described in ref. [S3] To obtain MIS/MIM structures, an upper Al electrode array was deposited on the poly(OFB-ThS) layer by thermal spraying through a shadow mask. The Al contact area was 0.5 mm^2. To improve the electrical contact for *UA (jF)* measurements, the bottom electrode was also thermally sputtered over the entire area of the non-planar Si substrate. Thickness control was carried out by spectral ellipsometry.

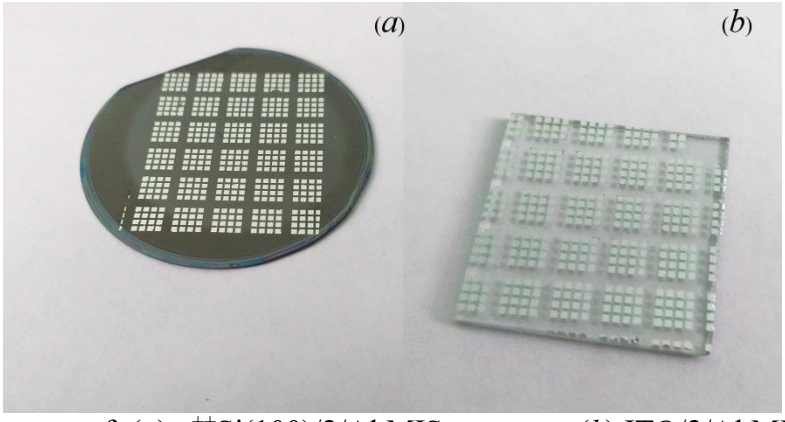

Figure S5. Images of: (*a*) p^{++}Si(100)/**3**/Al MIS structure, (*b*) ITO/**3**/Al MIM structure.

The MIS *UA (jF)* characteristics were measured using a Keithley 2400 electrometer. The different temperature range of 300 to 375K was set in the cell LTS420E from Linkam and temperature controller Linkam T95. The voltage ramp rate was 0.9 V/sec (Figure 2, main text)

Spectral Ellipsometry

The poly(OFB-ThS) film thickness (*d*) and refractive index were measured using an Ellips-1881 SAG spectral ellipsometer. The refractive index (*n*) and absorption coefficient (α) are shown in Figure S5. The optical constants of the poly(OFB-ThS) film were reconstructed from the multi-angle data by solving the inverse problem of ellipsometry by optimization methods for each photon energy independently. In the ultraviolet region, there are three peaks in *n* and α. The refractive index in the infrared region is close to that for similar organic films [S3]. The refractive index of the studied poly(OFB-ThS) **3** at the quantum energy of 1.1 eV is 1.49 (Figure S6). A film thickness of 26 nm was used for the memristor structure, p^{++}Si(100)/**3**/Al. For the Si(100)/**3**/Al structure, the film thickness of 110 nm was used to study the trapping charge transfer mechanism.

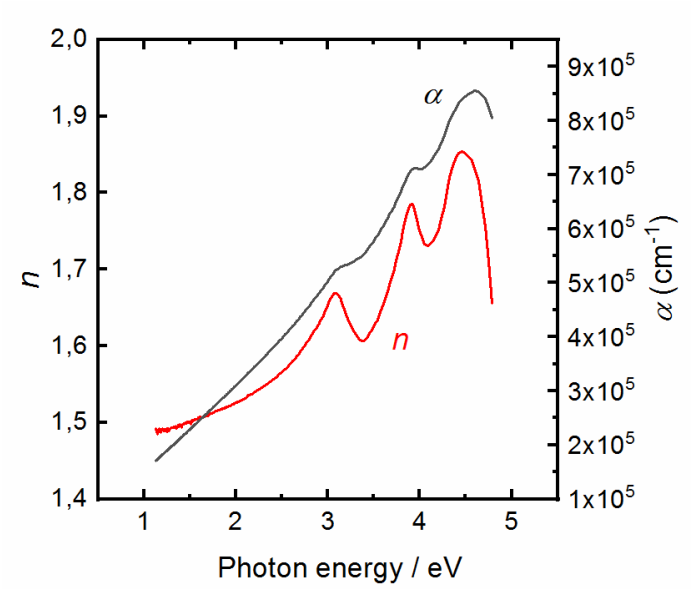

Figure S6. Refractive index (n) and absorption coefficient (α) of the poly(OFB-ThS) film deposited on p^{++}Si(100) wafer at different quantum energies

Charge transport in the poly(OFB-ThS) film: description with Frenkel model.

The charge transport mechanism in a dielectric with traps is given by the expression [S4]:

$$j = \frac{e}{a^2} P = eN^{2/3} P \qquad (1),$$

where j – current density, e – electron charge, a – average distance between traps, $N = a^{-3}$ – trap concentration and P – trap ionization probability.

The exponential dependence of current density on the electric field in the Frenkel effect is due to a decrease in the Coulomb barrier in the electric field. The trap ionization probability in the Frenkel model is described by the expression [S5]:

$$P = \nu \exp\left(-\frac{W - \left(\frac{e^3}{\pi \varepsilon_\infty \varepsilon_o} \right)^{1/2} \sqrt{F}}{kT} \right) \qquad (2),$$

where $\nu = W/h$ – attempt to escape factor, W – trap ionization energy, h – Planck constant, $\varepsilon_\infty = n^2$ – high-frequency permittivity, n – refractive index, ε_0 – dielectric constant, F – electric field, k – Boltzmann constant and T – temperature.

The experimental voltammetric (in j-F form) characteristics of p++Si(100)/**3**/Al memory device were simulated by the Frenkel model (Figure S6). The corresponding trap ionization energy (W) found in the simulation is 0.55 eV. We can then calculate the attempt to escape factor value using the Einstein relation: $\nu = W/h$. The value of the attempt to escape factor at the trap ionization energy of 0.55 eV is 1.3×10^{14} sec^{-1}. The high-frequency dielectric constant value

obtained from the simulation is ε_∞=19. On the other hand, the value of the high frequency dielectric constant can be obtained from the following expression: $\varepsilon_\infty = n^2 = (1.49)^2 = 2.22$.

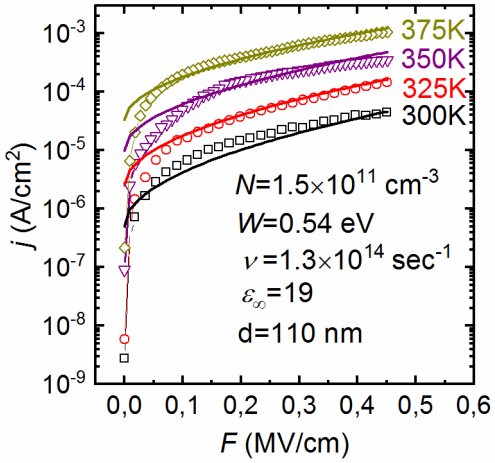

Figure S7. Voltammetric (in *j-F* coordinates) characteristics of the Si (100)/poly(OFB-ThS)/Al (d=110 nm) device at different temperatures (symbols) together with their simulations with the Frenkel model (solid curves)

Thus, the Frenkel effect does not describe the charge transport and trap ionization in the poly(OFB-ThS). Furthermore, the Frenkel effect predicts an immeasurably low trap concentration value N=1.5×10^{11} cm^{-3}. Note that the measurable trap concentration in inorganic dielectrics is in the range of 10^{18}-10^{21} cm^{-3} [S6].

References supplementary

S1 D. S. Odintsov, I. A. Os'kina, I. G. Irtegova and L. A. Shundrin, *Eur. J. Org. Chem*., 2023, **26**, e202300459.

S2 D. S. Odintsov, I. K. Shundrina, I. A. Os'kina, I. V. Oleynik, J. Beckmann and L. A. Shundrin, *Polym. Chem*., 2020, **11**, 2243.

S3 D. S. Odintsov, I. K. Shundrina, A. A. Gismatulin, I. A. Azarov, R. V. Andreev, V. A. Gritsenko and L. A. Shundrin, *J. Struct. Chem*., 2022, **63**, 1811 (*Zh. Strukt. Khim*., 2022, **63**, 101782).

S4 V. A. Gritsenko, T. V. Perevalov, V. A. Voronkovskii, A . A. Gismatulin, V. N. Kruchinin, V. Sh. Aliev, V. A. Pustovarov, I. P. Prosvirin and Y. Roizin, *ACS Appl. Mater. Interfaces*, 2018, **10**, 3769.

S5 J. Frenkel, *Phys. Rev*., 1938, **54**, 647.

S6 K. A. Nasyrov and V. A. Gritsenko, *Phys.-Usp*., 2013, **56**, 999 (*Usp. Fiz. Nauk*, 2013, **56**, 1099).